FUNDAMENTAL STUDY ON SAND STABILIZING AGENT INCORPORATING WITH NEW CHEMICAL MIXTURE

KONG KA MING

A project report submitted in partial fulfilment of the requirements for the award of Bachelor of Engineering (Honours) Civil Engineering

Lee Kong Chian Faculty of Engineering and Science
Universiti Tunku Abdul Rahman

APRIL 2021

DECLARATION

I hereby declare that this project report is based on my original work except for citations and quotations which have been duly acknowledged. I also declare that it has not been previously and concurrently submitted for any other degree or award at UTAR or other institutions.

Signature : 

Name : Kong Ka Ming

ID No. : 16UEB03466

Date : 09/05/2021

APPROVAL FOR SUBMISSION

I certify that this project report entitled **"FUNDAMENTAL STUDY ON SAND STABILIZING AGENT INCORPORATING WITH NEW CHEMICAL MIXTURE"** was prepared by **KONG KA MING** has met the required standard for submission in partial fulfilment of the requirements for the award of Bachelor of Engineering (Honours) Civil Engineering at Universiti Tunku Abdul Rahman.

Approved by,

Signature : 

Supervisor : Lee Foo Wei

Date : 09/05/2021

ACKNOWLEDGEMENTS

I would like to thank everyone who had contributed to the successful completion of this project. I want to express my sincere gratitude to my research supervisor, Dr Lee Foo Wei, for his beneficial advice, guidance, and precious patient throughout the research.

Besides, I would like to express my deepest gratitude to my parents and friends who helped and gave me kind support throughout the research. Also, I would like to appreciate senior course mate for the help, advice and experiences sharing throughout the research period.

Finally, I would love to treasure Ms Mandy So Shyun for the support, motivation, and cherish of the research project's smooth accomplishment.

ABSTRACT

Sand having poor geotechnical properties and the involvement of stabilization can modify it to fulfil construction purpose. The mixed sand stabilizer of hydrated lime, Class C fly ash, sodium silicate, and natural coir fibre was used for the geotechnical properties' enhancement and structure reinforcement to the sand. In this study, coir fibre was selected as the natural fibre for sand stabilization. Natural fibre stabilization is a cost-effective and environmentally sustainable way of enhancing sand properties. The laboratory tests of unconfined compression test and direct shear test were performed to determine and evaluate the effects of lime-fly ash-sodium silicate-coir fibre-reinforced sand. The varying proportion of coir fibre and different curing periods were selected for the tests to investigate the strength development. The laboratory test results showed that the lime-fly ash-sodium silicate-coir fibre-reinforced sand mixture could significantly enhance the geotechnical properties of sand. The incorporating of 1 % coir fibre reinforcement improves the structural stability of sand particles. The curing periods of 28 days and 56 days yield the desirable strength and highest strength value. The findings of the analysis can be used as a reference for sand reinforced engineering.

TABLE OF CONTENTS

LIST OF TABLES

LIST OF FIGURES

LIST OF SYMBOLS / ABBREVIATIONS

A	cross-sectional area, m^2
A_{inner}	inner cross-sectional area, m^2
A_0	initial cross-sectional area, m^2
A’	corrected cross-sectional area, m^2
C_g	coefficient of gradient
C_u	uniformity coefficient
c_u	undrained shear strength, kPa
c’	cohesive strength, kPa
D_r	relative density
D_{50}	mean effective diameter, mm
e_{max}	maximum void ratio
e_{min}	minimum void ratio
G_s	specific gravity, kg/m^3
h	height of specimen, m
L_0	initial length, mm
m	mass of specimen, kg
m_0	initial mass of specimen, kg
m_d	mass of solid of specimen, kg
N	axial load, kN
P	axial load, kN
q_t	split tensile strength, kPa
q_u	unconfined compressive strength, kPa
S_r	saturation, %
S_u	undrained shear strength, kPa
v	volume of specimen, m^3
ε	axial strain, %
τ	shear stress, kPa
ρ_b	bulk density, kg/m^3
ρ_d	dry density, kg/m^3
$(\rho_d)_{max}$	maximum dry density, kg/m^3
$(\rho_d)_{min}$	minimum dry density, kg/m^3

ΔH	horizontal displacement, mm
ΔL	change in length, mm
Δv	vertical displacement, mm
σ_n	normal stress, kPa
φ'	angle of internal friction, °

ASTM	American Society for Testing and Materials
BSCS	British Soil Classification System
Ca	calcium
CBR	California Bearing Ratio
CH	heavy clay
C-A-H	calcium aluminate hydrate
C-S-H	calcium silicate hydrate
CT	curing period
FA	fly ash
FSI	free swell index, %
kPa	kilopascal
LL	liquid limit, %
MDD	maximum dry density, kN/m^3
MH	heavy silt
Na_2SiO_3	sodium silicate
OMC	optimum moisture content, %
PI	plasticity index, %
PL	plastic limit, %
UCS	unconfined compressive strength, kPa
UCS_{max}	maximum unconfined compressive strength, kPa
UCT	Unconfined Compression Test
USCS	Unified Soil Classification System
USS	undrained shear strength, kPa
SEM	Scanning Electron Microscopy

CHAPTER 1

INTRODUCTION

1.1 General Introduction

Sand as one of the materials for geotechnical engineering construction are abundant, but high-quality sands are rare in most of the world. Engineers are obligated to explore the possibility to acquire the specified demand. Besides, it is urgent to gather the sufficient understanding and informative knowledge needed to enhance existing sand for geotechnical engineering application due to the ongoing urbanization, growth in population and the rapid development in the construction industry in recent years.

Sand stabilization is the blending and mixing process for sand enhancing physical and engineering properties to achieve some preordained targets. The enhancement of sand properties is a fundamental way to resolve numerous engineering problems. There is a plentiful operating course for sand stabilization such as chemical, physical, mechanical, biological and electrical. Among the various methods available for soil enhancement, chemical access for sand stabilization to improve geotechnical properties is catching more interest. The addition of soil stabilization and additives is a chemically enhancing approach that can promote sand with poor geotechnical properties to increase loading capacity and parameters for soil strength, decrease permeability, and modify microstructures. Adding additives to the sand may refine the gradation, plasticity or perform as a cementing binder of the sand (Ahmed and Radhia, 2019).

The geotechnical properties of the sand are essential not just in foundation material for projects but also as infrastructural substances for construction in slope stabilization, road, dams, embankment treatment, erosion control, coastal line and other works. Also, substantial interest increments in investigating soil enhancement plan that relies on the incorporation of stabilizing agents such as cementing agents, and synthetic or natural fibres for different applications are significantly witnessed within the engineering field

for geotechnical and material or pavements due to their low cost and convenience.

The intention for sand stabilization is mainly to enhance or refine the quality of sand to apply for any respective application or other purposes, while there are three goals for such stabilization. The first goal is to improve the strength parameters of the existing sand to enhance its load-bearing capacity. The second goal is for the dust control system to reduce site emissions since it is vital in meeting safety, health, and environmental requirements. The third goal is sand waterproofing; the practice of this is to withhold the calm or constructed strength of sands by restraining any infiltration or entry of surface water.

The adequate proportion of cement, fly ash, lime, or any other chemical-related combinations with sand can achieve the so-called additive stabilization. The degree of enhancement in the sand quality is relationally directed through the sand classification, type, and percentage of additives to be applied. The amounts of additives must depend upon the desired outcome; small additive amounts can refine the sand characteristics such as workability, gradation, and plasticity. A compatible proportion of it can improve strength and durability. The scheme of sand stabilizers can be marked as a traditional method and a non-traditional method (Eisazadeh, 2010). The use of cement, fly ash, lime, and bituminous materials are categorized as the traditional method. The use of polymer, enzymes, resin, silicates etc., is classified as the non-traditional method (Tingle, et al., 2007).

Another way of technique to effectively improve the strength properties, refine the liquefaction resistance and shorten the swelling potential of sand is by applying sand reinforcement with fibre. The advantages of using distributed short fibres are that it provides good strength properties and excellent strength with proper mixing. Thus, the combination of chemical additives for sand enhancing such as cement, fly ash, lime and polymer, and sand reinforcing with fibres such as coir, palm and banana etc., is taken into researching purposes. Jamsawang, et al. (2018) has reported that the cement-fibre-sand combination was favoured over a pure cemented case compared to the flexural performance. In other words, with such a combination case, it is much preferred than any

single course as the combined one has a more remarkable aspect of stability. It investigates value to explore further and comprehend the interactions and interrelations between sand particles, chemical additives and fibres, and the influencing properties of fibre such as size, softness, and strength parameters.

1.2 Importance of the Study

The value presented in this research is a supportive and contributing role to chemical stabilization techniques of lime, fly ash, sodium silicate, and different proportion of natural fibre reinforcement with coconut coir for the sand mixture. This study can be used as a guide to select the suitable proportion of reinforced coir fibres based on sand properties and the desired curing period for strength development.

1.3 Problem Statement

The use of cement, fly ash, lime and bituminous products as a traditional stabilizer have been researched accordingly, and the respective basic stabilization mechanisms have been determined (Obuzor, Kinuthia and Robinson, 2012). Currently, additives of non-traditional in liquid or powder form and natural fibres are keenly demanded in the construction industry. The stabilizing mechanism with the non-traditional one is not well determined. Also, the combination of chemical composition and fibre reinforcement will cause it difficult to measure the stabilizing mechanism and anticipate the performance outcome. Besides, evaluating the strength parameters of fibre-reinforced-stabilized sands on geotechnical properties focused on laboratory experimentation. The mixture combination of traditional material, non-traditional material and natural fibre is not sound research in the construction industry. Thus, it is significant to explore and examine the performance of sand stabilizer for such a combination.

1.4 Aim and Objectives

This project aims to study the performance of sand stabilizer for coir fibre reinforced-lime-fly ash-sand mixes with sodium silicate. The following objectives had been specified to achieve the aim of the research:

1. To compare the geotechnical properties of stabilized and non-stabilized sand, such as the Unconfined Compressive Strength (UCS) and shear strength parameters.
2. To study the strength behaviour of different proportion of reinforcing coir fibre with the lime-fly ash-sodium silicate-sand mixture on 7, 14, 21, 28 and 56 days.
3. To determine the effects of fibre mechanism to the strength development.

1.5 Scope and Limitation of the Study

The scope and limitation of the study are as follows:

1. The specimen used in this study was sand obtained from the campus of Universiti Tunku Abdul Rahman (UTAR), Bandar Sungai Long.
2. The chemical used, considered traditional additives, non-traditional additives, and natural fibres, was obtained from store purchasing in Malaysia.
3. The percentages of the chemical used in the mixture of sand additives were 5 % of lime, 25 % of Class C fly ash, 1 % of sodium silicate, and a different proportion of coir fibre content with 0 %, 0.5 %, 1.0 %, and 1.5 %. The curing periods are at 7, 14, 21, 28 and 56 days to determine the strength development of the treated sand.
4. The macro-structural study comprises the Unconfined Compression Test (UCT) and direct shear test.

1.6 Contribution of Study

The outcome of this research served as a reference for further studies of limitations and suggestion to the mixing combination of lime-fly ash-sodium silicate-sand mixture with the coir fibre reinforcement and investigation of laboratory tests.

1.7 Outline of Report

In Chapter 1 Introduction, the general introduction, the importance of the study, problem statement, aim and objectives, scope and limitation of the study, and the study's contribution are discussed.

Chapter 2 Literature Review discusses the type of material used, the properties and characteristics of the materials, type of soil stabilization, and the effect of combining mixture. All the information was based on the study, articles and research paper of professionals.

Chapter 3 Methodology and Work Plan discusses the methodology and work plan used in this project. The laboratory procedures and calculations, preparation of materials, mixing processes and experimental methods are involved.

Chapter 4 Result and Discussion discusses the result obtained of the lime-fly ash-sodium silicate-sand mixture at the varying proportion of coir fibre reinforcement on different designated curing periods. The optimum mixing coir fibre content and desired curing duration were discussed. The effects of the chemical combination and fibre mechanism were discussed based on the laboratory methods' results.

Chapter 5 Conclusion and Recommendation, it concludes the whole experiment project with the analysis and discussion of the results. The conclusion is made based on the objective to be accomplished. Also, several discussions have been made for the study in future purposes.

CHAPTER 2

LITERATURE REVIEW

2.1 Introduction

In Chapter 2, the size ranging of soil particles, type of stabilization method and fibre reinforcement were thoroughly reviewed. The standard for sieve analysis for sand particles was stated as well as the physical and mechanical properties of sand. The effect of chemical stabilization and physical reinforcement on the sand's geotechnical strength properties was included.

2.2 Sand

Sand is a loose granular material under unconsolidated condition, and the classification is based on its particle size. Sandy soil has low shear strength and cohesion in its geotechnical properties (Liu, et al., 2018). In the British Soil Classification System (BSCS), the sub-groups of sand consist of fine, medium, and coarse, ranging from 0.06 mm to 2 mm. Figure 2.1 shows the size ranges of clay, silt, sand and gravel, etc., as referring to BSCS. Sand can be separated from soils by sieve analysis into different size categories according to ASTM British Standards; sand category shall pass a 4.75-mm sieve (No. 4) and retain on a 0.075-mm (No. 200). Table 2.1 shows the sieve number classification for the sand particles. Table 2.2 shows the physical and mechanical properties of sand.

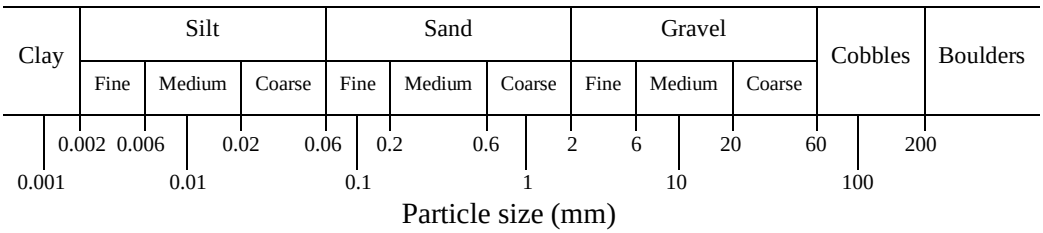

Figure 2.1: Size Ranging of Particles (Craig, 2004).

Table 2.1: ASTM Test Sieve Series for Sand Particles.

Sub-group of sand	Sieve number retaining (No.)	Sieve size (mm)
Coarse	10	2.00
Medium	40	0.475
Fine	200	0.075

Table 2.2: Physical and Mechanical Properties of Sand (Liu, et al., 2018).

Properties	**Values**
Specific gravity (g/ cm^3)	2.65
Dry density (Mg/ m^3)	1.34 – 1.66
Void ratio	0.590 – 0.970
Liquid limit (%)	Over 25
Plastic limit (%)	Over 20
Effective cohesion (kPa)	20 - 200

The mineral composition of the sand particles, such as the structural characteristics, strength properties of structural bonds, texture and water interaction, are influencing its properties. The sand itself is unstable, susceptible to environmental impact due to its loose structure, poorly graded and good hydraulic conductivity characteristic. Thus, it is essential to enhance its stability by reinforcing the sand mass (Liu, et al., 2018). One of the most influencing parameters for evaluating the sand properties is the void ratio, as it is correlating to the compressive strength, cohesion, shear strength and permeability. As shown in Table 2.2, the range for the void ratio of sand is considered high due to the high volume of voids within the sand mass. Consequently, enhancement of its cohesion by adopting a chemical stabilizer with lime and fly ash is a good countermeasure proven to improve sandy soil strength, while void ratio minimization can be achieved by fibre reinforcement (Vizcarra, Casagrande and da Motta, 2014).

2.3 Chemical Stabilization

Chemical stabilizing agents such as Portland cement, lime, fly ash is used for chemical stabilization that blend with sand. These agents are commonly used to bind the soil aggregates together effectively to achieve properties binders; they are also known as the potential binders to enhance loading capacity, stress capability, distributing characteristics, and control the rate of shrinkage and swelling (Garber and Hoel, 2009). The chemical reaction often applied and performed on natural soil treatment with chemical admixture and the respective chemical compound (Huat, Maail and Mohamed, 2005). The modification and enhancement with chemical reaction can contribute to sand's physical and engineering properties, such as volume adherence and strength. Nonetheless, this approach's adverse effect may consist of negative effects that cause high stiffness and brittleness (Bahar, Benazzoug & Kenai, 2004).

Moreover, the chemical bonding forces that develop between the particles in such aggregation would become more robust. Huat, Maail and Mohamed (2005) mentioned that the different stabilizer type would result in other characteristics and chemical bonding forces. Various factors affect the physical and mechanical properties, mainly the properties of the base material. Manipulating factors that affect strength development is influenced by the type and percentage of admixture, moisture content, compaction method, mixing procedure, condition and period of the curing process, humidity and mineral composition. Stabilized sand is the end product of "stabilization", the chemical admixture of "binders" or "stabilizer" added to any existing sand is a ground enhancing technique to improve its strength and reduce compressibility (Rafizul, Assaduzzaman and Alamgir, 2012).

2.3.1 Effect on Geotechnical Properties with Chemical Processes

Thyagaraj, et al. (2012) stated that soil's geotechnical properties were improved with the change in microstructure through 4 reactions. Olinic and Olinic (2016) further illustrated that the critical responses were carbonation, exchange of cation, flocculation-agglomeration and pozzolanic reaction. Cheng, et al. (2018) mentioned that the values of the compression strength and permeability went up due to the reduction of plasticity index (PI) and free swell index (FSI) developed by flocculation. Another critical parameter to achieve long-term compressive

strength (q_u) and split tensile strength (q_t) is the curing period as for the completion of the pozzolanic reaction (AI-Swaidani, Hammoud and Meziab, 2016). An effective way to reduce the swell potential of lime stabilized soil is to extend the curing period.

2.4 Lime Stabilization

The formation of lime is through the calcination process of limestone in a lime kiln at or above 1100 degrees Celsius. Calcium limestone consists of the chemical compound of calcium oxide or quicklime; quicklime, in turn, contact water; a hydraulic reaction to produce hydrated lime (calcium hydroxide) process is called slaking of lime. Also, lime is the traditional stabilizer used for a long history in the construction field. Joe and Rajesh (2015) mentioned that large quantities of these materials such as lime, concrete and mortar are still involved in the construction activity in building and engineering materials and as chemical raw material. Krithiga, et al. (2016) illustrated that the reaction of lime and fly ash with fine-grained soil led to reduction of plasticity and increase of workability and mechanical behaviour of soil. The primary aim of the chemical reaction obtained from the mixture of lime with sandy soil is to gain strength. There are two interest phases for such chemical reaction, with both immediate reacting responses and long-term benefits.

The exchange of cation within a chemical reaction brings out a direct change in sand component texture and properties of sand. The high pH value compared to the surrounding ground cause the pozzolanic reaction occurs between the free Ca +2 cation and the dissolved silica and alumina. Besides, sand mixture and lime compaction must be well compacted to prevent any undesirable cementation problem (Holt, 2010). Lime-treated specimens were indicated as a practical approach for increment in strength, durability and workability (Jawad, et al., 2014). However, the authors further mentioned some inherent disadvantages such as carbonation, sulphate attack, and environmental impact that may occur within a lime treatment. Table 2.3 shows the list of summarizing conducted research referred to a Ca-based stabilizer material for different soil across the world.

Table 2.3: A Concise List of Research Examined on Ca-Based Stabilizer Material for Different Soil Across the World.

Soil Properties	Referencing Authors			
	Ma, Cao and Yuan (2018)	Buhler and Cerato (2007)	Zumrawi and Babikir (2017)	Baldovino, et al. (2019)
Location of soil	China, Hefei, Anhui	USA, Idabel, Oklahoma	Sudan, Khartoum	Brazil, Curitiba
G_s	2.71	-	2.64	2.71
LL (%)	42.8	79	76	53
PL (%)	22	25	24	32
PI (%)	20.8	54	52	21
Activity	-	1.30	1.3	< 1
USCS	MH	CH	CH	MH
MDD (kN/m^3)	17.3	-	1.49	13.8
OMC (%)	18.9	-	26.0	28.5
Type of stabilizer	FA, S & B	L, CFA	FA	L
Optimum amount	10 % of FA + 8 % of S + 0.4 % of B	5, 10, 15 and 20 % of L and Class C FA each	10 % of FA (FA: SiO_2 is 54 % alumina 34 % of CaO is 3.6 %)	9 % of L
Properties improved	PI ↓, LL ↓, PL ↑, UCS ↑ = 345 to 900 kPa (with 0.4 % Ba fibres)	Shrinkage ↓ = maximum at 20 % lime	P_s ↓ (50 % to 70 %) at 25 % of F, P_s ↓ (90 %), UCS ↑ (almost 100 %)	UCS (by 75 %) Porosity ↓, MDD ↑

Note (1):

'G_s' represents Specific Gravity; 'PL' represents Plastic Limit; 'LL' represents Liquid Limit; 'PI' represents Plastic Index; 'USCS' represents Unified Soil

Classification System; ‘MDD’ represents Moisture Dry Density; ‘OMC’ represents Optimum Moisture Content.

Note (2):
‘B’ represents Basalt Fibre; ‘MH’ represents Heavy Silt, ‘CH’ represents Heavy Clay, ‘FA' represents Fly Ash; S represents sand; 'L' represents lime; ‘UCS’ represents Unconfined Compressive Strength.

Note (3):
↑ represents a decrease; ↓ represents an increase in the corresponding property.

2.5 Fly Ash Stabilization

The by-product from coal-burning is fly ash. Two classes of fly ash are Class C and Class F. For Class C fly ash, has much more self-cementing properties than Class F, approximately 30 % more CaO content, and it is suitable as a substitute for mass production concrete for Portland cement. The self-cementing properties allow it to stabilize and strengthen the poor quality of sand. On the other hand, even though Class F has a meagre benefit in cementing, combining it with additives such as hydrated lime, quicklime, or cement can create additional cementitious compound’s direct purpose.

2.6 Effect of Fly Ash Percentage

Simatupang, et al. (2020) reported that the enhancement in the maximum unconfined compressive strength (UCS_{max}) is due to the bonding formed by FA; the self-hardening process during curing will cause the sand particles’ bonding to become stronger over time as the FA content increase. Harichane, Ghrici and Kenai, (2011) mentioned a similar statement and showed that the strength enhances as the FA content increases.

2.7 Fibre Reinforcement

Unconventional soil stabilizers such as fibre reinforcement with banana and sodium silicate can be applied to unsuitable soil for the construction field. Kaniraj and Havanagi (2001) illustrated a substantial enhancement in shear strength using cement-fly ash-fibre with sand mixture combination. Their

results showed that both cemented and uncemented sand's peak and ultimate strength have a visible improvement with the reinforced fibre. Haghi, Arabani and Veis Karami (2006) reported a significant influence on engineering properties and stabilization of clayey sand with polyamide fibre as an admixture. Ravindran, et al. (2019) declared that the increase of banana fibre content could improve the PI, shear strength, UCS, CBR and split-tensile strength while stabilized with sodium silicate. Table 2.4 listed all the increased result in each geotechnical parameter with the application of 0.5 % banana fibre reinforcement.

Table 2.4: Results of Banana Fibre-Reinforced Soil (Ravindran, et al., 2019).

Result of laboratory tests with 0.5 % of banana fibre	Percentage increased (%)
Unconfined compressive strength	445
Shear strength	80
Split tensile strength	194
Soaked California Bearing Ratio	1083

Fibre reinforcement provides a convenient mixing procedure, good strength properties and ecological potential; this method is straightforward and effective when discrete and randomly distributed fibres (Liu, et al., 2018). Shukla (2017) stated that the outcome of the direct shear test on with or without the fibre reinforcement is by the increment of its peak shear strength and degree limitation of decrement in post-peak shear resistance.

2.7.1 Effect of Fibre Content on Unconfined Compressive Strength

Based on Sadek, Najjar and Abboud (2013), as shown in Figure 2.2, it indicates a clear improvement in the composite specimen's performance stabilized with 0.5 % cement and fibre reinforced in the range of 0 % to 1 %. The results presented that the UCS had improved approximately ten times the specimens without fibre reinforcement. The authors further stated that the UCS of the specimens enhanced with the increase of fibre content.

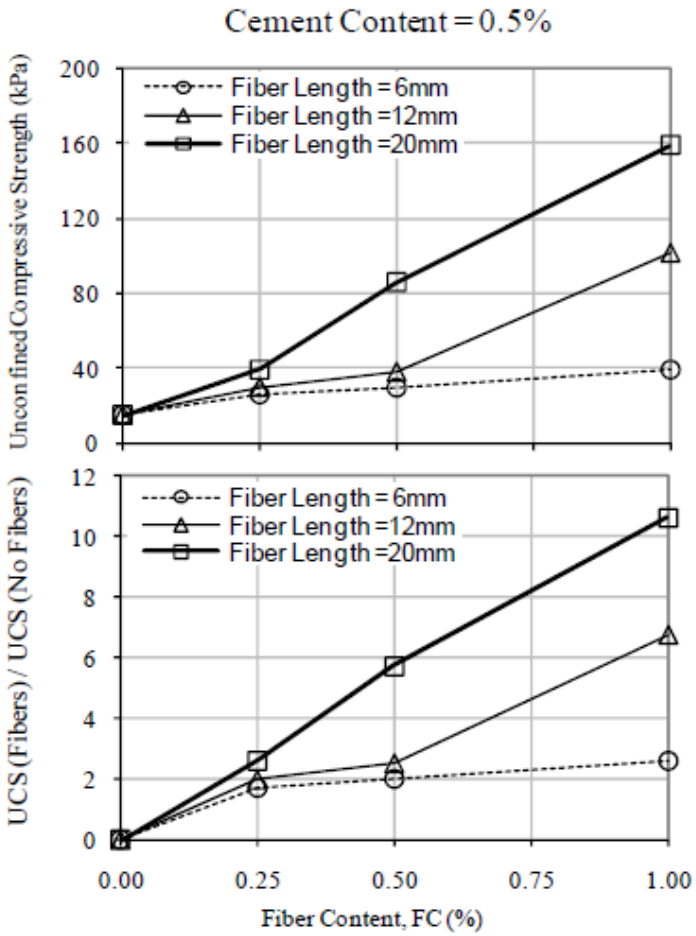

Figure 2.2: Improvement in UCS for Cement Content of 0.5 % (Sadek, Najjar and Abboud, 2013).

2.7.2 Coir Fibre

Coir fibre belongs to the hard-structural fibres group, and it is an essential commercial product obtained from the husk of a coconut. The coir fibre's elasticity allows it to be twisted and curled without breaking its structure (Subramani and Udayakumar, 2016). There is a reduction of plasticity and increment of hydraulic conductivity with the addition of fibre. Coir material is very cheap and easy to purchase, and it is environmentally friendly as it is biodegradable. The authors tested various CBR values and UCT conducted on coir fibre reinforced soil (0.25 %, 0.50 %, 0.75 % and 1.0% fibre content) under soaked and unsoaked condition. The authors concluded that with the percentage increase of fibre, the strength, CBR and UCS values of soil-coir fibre mix would increase also, and the optimum value was 0.5 % of coir fibre.

2.8 Sodium Silicate

The process of heating sand with the extra amount of alkali will produce sodium silicate. The blending of silicon dioxide with sodium carbonate and the development of carbon dioxide will also produce sodium silicate (Ravindran, et al., 2019). The appearance of sodium silicate is known as liquid glass. Kazemian, et al. (2012) explored that the combination of cement and sodium silicate is suitable for soil strengthening and moisture content reduction to stabilize organic soil. The bonding force introduced between soil particles by the soil stabilization with sodium silicate, thereby limiting particles rotation as sand particles typically appear to rotate at the fibre-soil interface (Shukla, 2017).

2.9 Summary

The soil stabilization and strength enhancement involve lime stabilization, fly ash stabilization, sodium silicate stabilization, and coir fibre reinforcement. The characteristics of sand, such as its loose structure, poorly graded and good hydraulic conductivity, lead it to become unstable and susceptible to environmental impact. Consequently, sand stabilization and reinforcement are needed to improve its geotechnical properties, such as the unconfined compressive strength, cohesive strength, angle of internal friction. Lime, fly ash, sodium silicate, and coir fibre reinforcement are an excellent combination to enhance the strength parameters while minimizing the void ratio. The involvement of lime and fly ash will cause carbonation, exchange of cation, flocculation-agglomeration and pozzolanic reaction to improve the strength properties. The response of lime and fly ash reduces plasticity, increases the soil's workability and mechanical behaviour, and provides long-term benefits.

However, certain inherent drawbacks, such as carbonation, sulphate strike, and environmental effects, can occur during the lime treatment process. The bonding produced by fly ash improves the overall unconfined compressive strength. During the curing period, the self-hardening process causes the sand particles' bonding to become stronger over time as the fly ash content increases. Coir material is affordable and convenient to produce, and it is environmentally safe because it is biodegradable. For the elasticity of the coir fabric, it can be twisted and curled without destroying its shape. As the percentage of fibre increases, so would the strength, CBR, and UCS values of the soil-coir fibre

mixture. The bonding force introduced between soil particles by sodium silicate soil stabilization, thus reducing particle rotation as sand particles appear to rotate at the fibre-soil interface. Hence, it can be applying the mixture of reinforced coir fibre-lime-fly ash-sodium silicate-sand to investigate further and enhance the sand’s geotechnical properties.

CHAPTER 3

METHODOLOGY AND WORK PLAN

3.1 Introduction

This chapter will cover the detailed description of the project methodology and work plan used to carry out the laboratory tests. The preparation of materials, the combination of the sand specimens, experiments' procedures and the related calculations will be discussed in the subsections and the sub-subsections below.

3.1.1 Experimental Methods

In this study, an unconfined compression test (UCT) and direct shear test were carried out to determine specimens' performance incorporating the coir fibre reinforced-lime-fly ash-sand mixes with sodium silicate. The percentages of fibre content are 0 %, 0.5 %, 1.0 % and 1.5 %. While the curing periods of 7 days, 14 days, 21 days, 28 days and 56 days had been proposed for this investigation. For the mixing phase of all sand specimens, the moisture content of 30 % was used and favourable to the strength development purposes. The untreated and unreinforced specimens were selected as the base references.

In preparing all specimens, dry sand and proposed fibre content were mixed on a tray in small accumulative proportion by hand to acquire a uniform mixture. The proposed content of lime-fly ash-sodium silicate and water were incorporated into the sand specimen mixture. The mixture was constantly stirred throughout the mixing phase to ensure it had the complete chemical reaction coverage on the sands' surface area. In the meantime, the thorough mixing of coir fibres was provided to achieve a final mixture. Eventually, the sand mixtures were prepared for the specimens to commence the laboratory tests of UCT and direct shear test.

3.1.2 Flow of Work Plan

Figure 3.1 shows the flowchart of the overall experiment.

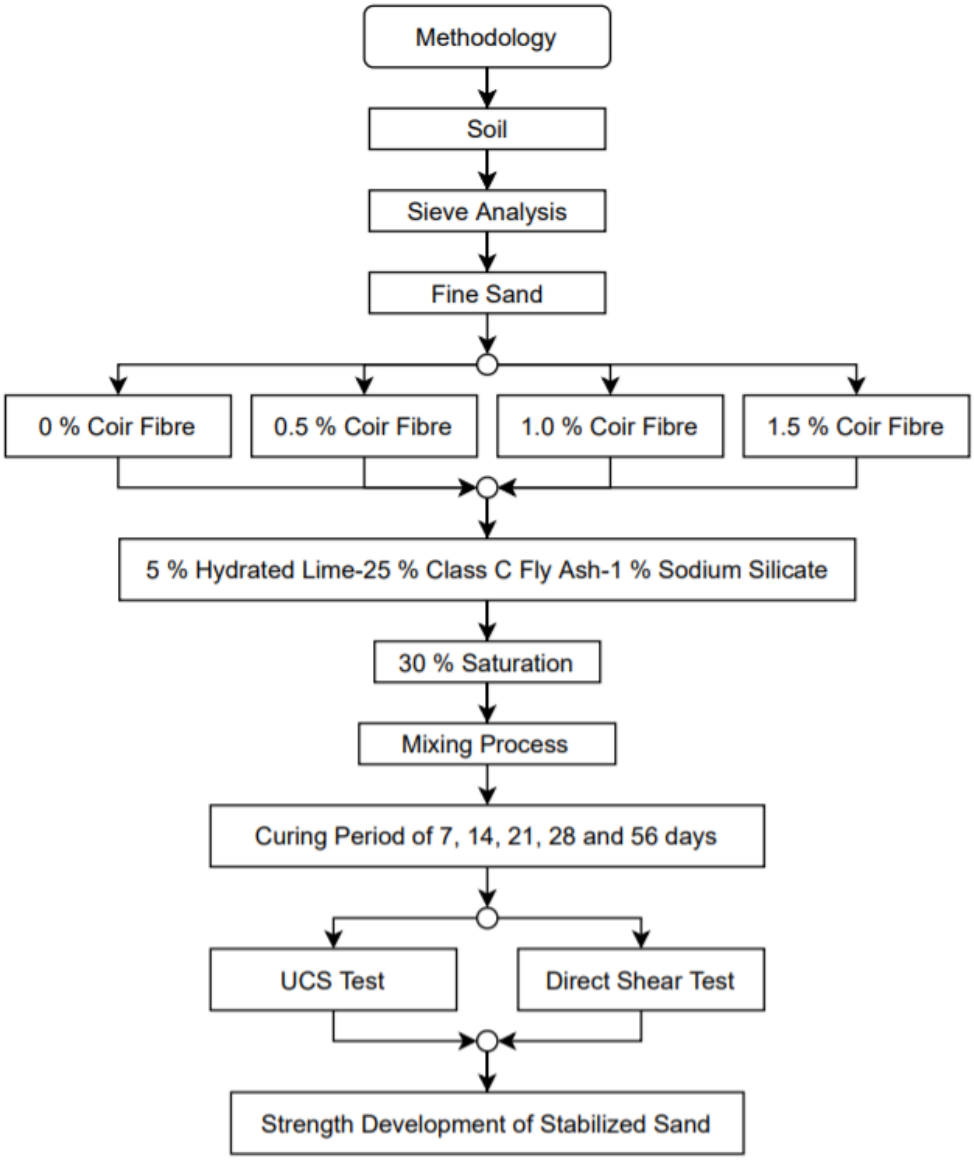

Figure 3.1: Flowchart of the Experimental Program.

3.2 Materials

The materials used in this project include hydrated lime powder, Class C fly ash, sodium silicate, coir fibre, water and sand.

3.2.1 Classification of Sand

In this study, sand was obtained from UTAR. The dried soil sample will be placed on top of a stacked set of sieves for sieve analysis. The sand sample with

the mean effective diameter (D_{50}) is 0.32 mm. The void ratio is range from 0.583 to 0.965. Figure 3.2 shows the sample of sieve stacking for the sieve analysis. Based on Table 3.1, the sieved sample for sand particles will be used at which the soil passes through sieve number 4 and retaining at sieve number 200 on the stack.

Figure 3.2: Sample of Set Sieves.

Table 3.1: Unified Soil Classification by Grain Size.

#4 [# 10 for AASHTO)	4.75 mm (2.0 mm)	~0.2 in (~0.08 in)		Coarse Grained
			Coarse Sand	
#10	2.0 mm	~0.08 in		
			Medium **Sand**	
#40	0.425 mm	~0.017 in		
			Fine Sand	
#200	**0.075 mm**	**~0.003 in**		
			Silt	Fine Grained
	0.002 mm to 0.005 mm			
			Clay	

3.2.2 Lime, Fly Ash and Sodium Silicate

Hydrated lime and sodium silicate were purchased in supplying store within Malaysia for the experiment. Class C FA with more cementing properties was chosen to produce a good outcome for the specimen's geotechnical properties. Figure 3.3, Figure 3.4 and Figure 3.5 show the experimental materials of

hydrated lime powder, Class C fly ash, and sodium silicate in powder form, respectively.

Figure 3.3: Hydrated Lime Powder.

Figure 3.4: Class C Fly Ash.

Figure 3.5: Sodium Silicate.

3.2.3 Coir Fibre

Coconut coir is a natural fibre extracted from the husk of the coconut. The advantage of this natural fibre is related to its cheap cost and improved strength

of the specimen, locally available and eco-friendly. Table 3.2 shows the properties of coir fibre in the specimen. Figure 3.6 shows the coir fibre to be used in experimental tests.

Table 3.2: Properties of Coir Fibre.

Description	Value
Diameter	0.5 mm
Length	3 to 5 cm
Specific gravity	1.3

Figure 3.6: Coir Fibre.

3.2.4 Water

Tap water is used for the mixing purpose, and the water-to-sand weight ratio for this project is fixed in the proportion of 0.30. Fly ash reacts with lime at ambient temperature in the presence of moisture to form a compound with cementitious properties.

3.3 Bulk Density

The bulk density is represented as the total soil mass of the specimen per unit volume.

$$\rho_b = \frac{m}{v} \tag{3.1}$$

where

ρ_b = bulk density, kg/m^3

m = total mass of specimen, kg

v = volume of specimen, m^3

3.4 Dry Density

The dry density is represented as the dry solid mass of the specimen per unit volume.

$$\rho_d = \frac{m_d}{v} \tag{3.2}$$

where

ρ_d = dry density, kg/m^3

m_d = mass of solid of specimen, kg

v = volume of specimen, m^3

3.5 Combination of Specimen Mixtures.

Table 3.3 listed the combination of stabilizers for sand specimens in percentages. The mixing procedures are then proceeded to obtain a complete set of specimens for curing purpose. The curing period was set to 7, 14, 21, 28 and 56 days, and the saturation percentage for all set was fixed to 30 % of the specimen dry weight. Experimental tests will be carried out with the reach of each respective curing period.

Table 3.3: Percentage Combination of Stabilizers into Sand Specimens.

Specimens	Combination of Mixture						
	Saturation, Sr (%)	Lime (%)	Sodium Silicate, Na_2SiO_3 (%)	Coir Fibre (%)	Fly Ash, FA(%)	Sand (%)	Curing Period, CT (days)
S0	0	0	0	0	0	100	-
S1	30	5	1	0	25	69	7
S2		5	1	0.5	25	68.5	
S3		5	1	1.0	25	68.0	
S4		5	1	1.5	25	67.5	
S5		5	1	0	25	69	14
S6		5	1	0.5	25	68.5	
S7		5	1	1.0	25	68.0	
S8		5	1	1.5	25	67.5	
S9		5	1	0	25	69	21
S10		5	1	0.5	25	68.5	
S11		5	1	1.0	25	68.0	
S12		5	1	1.5	25	67.5	
S13		5	1	0	25	69	28
S14		5	1	0.5	25	68.5	
S15		5	1	1.0	25	68.0	
S16		5	1	1.5	25	67.5	
S17		5	1	0	25	69	56
S18		5	1	0.5	25	68.5	
S19		5	1	1.0	25	68.0	
S20		5	1	1.5	25	67.5	

3.6 Unconfined Compression Test

This test is referencing ASTM D2166, Standard Test Method for UCS of Cohesive Soil. This test's main intention is to determine the UCS; the compressive load will be applied to the cylindrical specimen so that no drainage occurs during the shear. The UCS is represented as the maximum load obtained

per unit area at 15% of axial strain. The UCS is then used to calculate the USS of the sand. (3.3) is the formula for calculating the undrained shear strength, c_u of the specimen.

$$S_u = \frac{q_u}{2} \tag{3.3}$$

where

S_u = undrained shear strength, kPa

q_u = unconfined compressive strength, kPa

Stabilizers were added in percentage based on the dry weight of the sand specimen that according to Table 3.3. The specimen is prepared in a cylindrically shaped mould with a diameter of 50 mm and length of 100 mm.

3.6.1 Test Procedure for Unconfined Compression Test

Procedure steps are listed as follow:

1. Construct a cylindrical shaped specimen with 50 mm diameter and 100 mm height using a mould.
2. Position and centre the specimen onto the bottom plate of the compression device with the electric load cell.
3. Set all the dial gauge readings to zero after assuring the upper plate contacts the specimen.
4. Apply the load to yield an axial strain (rate of 0.5 % to 2 % per minute). Record the load cell reading and deformation dial readings on the datasheet at every 20 divisions on the deformation dial.
5. Stop the load applying if the following conditions are achieved,
    i. Appreciable load decrement, or
    ii. Four continuous readings on load cell dial, or
    iii. Exceeding of 15 % strain deformations.
6. Sketch to illustrate the specimen failure.
7. Repetition on test procedures (2) to (6) for other specimens.

3.6.2 The calculation for the Unconfined Compression Test

The calculation steps and formula are listed below:

I. Calculations

1. Convert the deformation and load cell reading (unit) to kN units, respectively. Conversion factors are based on the testing model used.
2. Calculate the corrected cross-sectional area, A' (m^2), of the specimen:

$$A' = \frac{A_0}{1 - \varepsilon} \tag{3.4}$$

where

A_0 = initial cross-sectional area of the specimen, m^2

ε = axial strain, equal to $\Delta L/L_0$

whereby,

L_0 = initial length of the specimen, mm

ΔL = change in length evaluated by the deformation gauge, mm

3. Compute the specimen stress:

$$\sigma = \frac{P}{A'} \tag{3.5}$$

where

P = axial load, kN

A' = corrected cross-sectional area, m^2

II. Test Data:

Develop a UCS test Excel Data Sheet and sketch the failure mode of the specimen.

III. Plotting:

a) Plot the stress (σ) versus strain (ε) graph. Determine the UCS (q_u).

3.7 Direct Shear Test

This test is according to British Standard 1377- Part 7: Shear Strength Tests. Direct Shear Test is a quick and cheap test. It is used to investigate the shear strength properties of dry sand. The benefits of using Direct Shear Tests are simple to carry out; both peak and shear strength can be determined and applied to all soil types. The shear strength properties obtained are used to analyze the slope's stability and determine the foundations' bearing capacity.

3.7.1 Test Procedure for Direct Shear Test

Procedure steps are listed as follow:

1. Measure and calculate the inner dimension and inner area (A_{inner}) of the shear box, respectively.
2. Weight and record the initial mass of the specimens.
3. Assemble all the parts of the shear box.
4. Compact the specimen in the mould after watering it to optimum moisture condition (OMC).
5. Transfer the specimen carefully into the shear box.
6. Position the loading plate onto the upper porous plate. Record the weight of the loading carrier place.
7. Position and set the readings on dial gauges to zero. Unscrew the alignment screws that holds two halves of the shear box.
8. Tighten up the remaining two transversely opposite screws until a small gap is attained. The purpose is to decrease the frictional force.
9. Apply the axial stress. Wait for the dial gauges until an indication of constant reading is obtained, then reset the value in the dial gauge to zero. This only happens when there is any vertical displacement.
10. Check and remove the screws and start up the motor to produce a specific constant shearing rate.

11. Take all the readings such as the shear displacement, shear load and vertical displacement (every ten incremental division).
12. Stop the test when the shear load start to decrease or remains constant at least three readings.

3.7.2 Calculation for Direct Shear Test

The calculation steps and formula are listed below:

I. Calculations

1. Calculate the bulk density of the specimen:

$$\rho = \frac{m_0}{A\ x\ h} \tag{3.6}$$

where

ρ = bulk density of specimen, kg/m^3

m_0 = initial mass of specimen, kg

A = cross-sectional area of the specimen, m^2

h = height of specimen, m

2. Calculate the relative density of specimen:

$$D_r = \frac{(\rho_d)_{max}}{\rho_d}\left[\frac{\rho_d\ -\ (\rho_d)_{min}}{(\rho_d)_{max} - (\rho_d)_{min}}\right] x\ 100\ \% \tag{3.7}$$

where

D_r = relative density of the specimen

ρ_d = dry density, kg/m^3

$(\rho_d)_{max}$ = maximum dry density, kg/m^3

$(\rho_d)_{min}$ = minimum dry density, kg/m^3

3. Calculate the normal stress:

$$\sigma_n = \frac{N}{A} + Intial\ stress \tag{3.8}$$

where

σ_n = normal stress, kPa

N = axial load, kN

A = cross-sectional area, m^2

Initial stress = 9.81 kPa

4. Calculate the shear stress:

$$\tau = \frac{F}{A} \tag{3.9}$$

where

τ = shear stress, kPa

F = recorded shear force derived from the proving ring, kN

A = cross-sectional area, m^2

II. Plotting:

a) Plot the stress (τ) versus horizontal displacement (ΔH) graph for each applied normal stress, and identify the shear stress at failure (τ_f).

b) Plot the vertical displacement (Δv) versus relative horizontal displacement(ΔH) graph for each applied normal stress, and identify whether the specimen dilate or contract.

c) Plot the Mohr-Coulomb failure envelope (shear stress at failure versus normal stress). Determine the cohesion (c') and friction angle (φ') of the specimen.

3.8 Summary

There are 40 stabilized sand specimens of mixed proportion and two non-stabilized sand specimens in this project. The mix proportion of 5 % hydrated lime-25 % Class C fly ash-1 % sodium silicate was fixed for specimens S1 to S20 for both unconfined compression test and direct shear test. Specimen S0 for both laboratory tests was the non-stabilized specimen of 100 % sand containing for the base reference purpose. The standard of UCT is referencing ASTM

D2166, Standard Test Method for UCS of Cohesive Soil, while the standard of direct shear test is referring to British Standard 1377- Part 7: Shear Strength Tests. The varying proportions of reinforcing fibre content were 0 %, 0.5 %, 1.0 % and 1.5 %. The curing periods were set as 7 days, 14 days, 21 days, 28 days and 56 days. The coir fibre diameter is approximately 0.5 mm thick, and its length is ranged from 3 cm to 5 cm. The saturation percentage for all specimens was 30 % of the dry sand weight.

CHAPTER 4

RESULT AND DISCUSSION

4.1 Introduction

In this chapter, result from analysis and discussion will be made based on the unconfined compression test and direct shear test that has been conducted on specimens with varying percentages of coir fibre and five designated curing periods. In this project, a total of 42 soil samples were prepared and listed with specimen code name distinctly for the investigation on strength parameters such as unconfined compressive strength, cohesion, and angle of internal friction. The behaviour of strength development in each specimen will be determined, evaluated, and further discussed to support this project's findings.

4.2 Mixed Proportion of Sand Specimen

Table 3.3 shows the mixing combination in percentages by referring to the weight of the sand sample prepared. The percentage value of hydrated lime, sodium silicate, and fly ash were fixed at 5 %, 1 %, and 25 %, respectively, for all the specimens except for specimen S0 which has been assigned for the base referencing in favour of comparing and evaluating the strength development to other specimens during the curing process. Since the involvement of the lime-fly ash-sodium silicate mixture represents the controlled variable, with such specimen combination, it can be identified that the fibre content reinforcement was the manipulated variable. At the same time, the curing period executed the progress of strength development. Table 4.1 display the grain size distribution of sand. Table 4.2 states the property parameters of the experimental sand used in each specimen.

Table 4.1: Grain Size Distribution of Sand.

Grain size (mm)	Weight percentage content (%)
2 – 1	0.2
1 – 0.5	16.9
0.5 – 0.25	49.1
0.25 – 0.10	31.5
0.1 – 0.075	2.3

Table 4.2: Property Parameters of Experimental Sand.

Maximum density, ρ_{max} (g/cm^3)	1.67
Minimum density, ρ_{min} (g/cm^3)	1.36
Maximum void ratio, e_{max}	0.965
Minimum void ratio, e_{min}	0.583
Median diameter, D_{50} (mm)	0.32
Uniformity coefficient, C_u	2.76
Coefficient of gradation, C_g	1.11
Specific gravity, G_s	2.65

4.3 Unconfined Compression Test

The unconfined compression test was used to derive the unconfined compressive strength; the purpose of this laboratory test aims to determine maximum axial compressive stress sustained by specimens that bear under zero confining stress. Table 4.3 displays the result of unconfined compressive strength in kilopascal (kPa) of each tested specimen with the varied curing period. In this study, the untreated specimen S0 failed to have shape development and contribution into the unconfined compression test; this is mainly due to the imperfect nature of cohesive force within the sand particles. The chemically-treated specimens were able to form the desired shape after the moulding procedure.

The UCS of specimens reinforced with fibre content of 0 %, 0.5 %, 1.0 %, and 1.5 % are 69.66 kPa, 121.91 kPa, 230.41 kPa, and 165.90 kPa, respectively, on the 7th day of curing period. As referring to Table 4.3, it can be

distinguished clearly that the UCS of the specimen was enhanced by the chemically treated material of lime-fly ash-sodium silicate and the physically reinforced component of coir fibre. Also, a column inside Table 4.3 indicates the strength improvement with percentage division by dividing the reinforced specimen set to the unreinforced specimen under the same curing period. The justification for using the fibre-unreinforced specimen S1, S5, S9, S13, and S17 as the denominator in calculating the UCS improvement mainly acts as the respective reference's tendency much comparable manner and concise way. Consequently, the value of strength improvement data for the fibre-unreinforced specimen is equal to 0. While viewing the percentages in strength improvement, the positive value outcome further expresses each specimen's significant strength development. Thus, the strength development is influenced by the amount of fibre content and the curing period's time factor.

Table 4.3: Unconfined Compressive Strength of Sand Specimens.

Specimens	Dry density (g/ cm^3)	Coir fibre (%)	UCS (kPa)	Strength improvement by percentage (%)	Curing period, CT (days)
S0	1.52	0	-	-	-
S1	1.52	0	69.66	0	7
S2	1.52	0.5	121.91	75.01	
S3	1.52	1.0	230.41	230.76	
S4	1.52	1.5	165.90	138.16	
S5	1.52	0	77.33	0	14
S6	1.52	0.5	153.61	98.64	
S7	1.52	1.0	324.88	320.12	
S8	1.52	1.5	195.76	153.15	
S9	1.52	0	101.30	0	21
S10	1.52	0.5	207.37	104.71	
S11	1.52	1.0	396.35	291.26	
S12	1.52	1.5	309.29	205.32	
S13	1.52	0	116.49	0	28
S14	1.52	0.5	282.02	142.10	
S15	1.52	1.0	495.44	325.31	
S16	1.52	1.5	411.36	253.13	
S17	1.52	0	121.15	0	56
S18	1.52	0.5	287.66	137.44	
S19	1.52	1.0	535.07	341.66	
S20	1.52	1.5	460.72	280.29	

4.3.1 Stress-Strain Curves Analysis

The stress-strain curve is applied to present the relationship between the stress and strain of the sample. The curves were generated by inserting the data into the Microsoft Excel software obtained from the UCT, where specimens experienced axial load from the top surface area, and stress and strain measurements are taken continuously and simultaneously. The curves provide

a clear view of the treated sand sample's deformation in response to compressive load and determine the maximum unconfined compressive strength while selecting the peak point of the curve itself.

Figure 4.1, Figure 4.2, Figure 4.3 and Figure 4.4 show the axial stress-strain curves of specimens with 0 %, 0.5 %, 1.0 %, and 1.5 % of coir fibre reinforcement, respectively, on five different designated curing period. The lime-fly ash-sodium silicate mixes specimens either without or without coir fibre reinforcement be likely to soften after reaching an apparent peak value. Besides, the specimens are primarily in a ductile failure state due to the ductile overload beyond its strength's limit. In the stress-strain curves, the peak value represents the unconfined compressive strengths of the treated sand specimens. As seen in the stress-strain curve, the axial stress increases with the advancing of axial strain; axial stress value increments will stop when the peak value has been reached. As the peak value had been obtained, the axial stress value increases no more but decreases to a stable value. Besides, the specimens have a more considerable value in residual strength as the curing period is getting longer. When taking into an overall view on all of the four stress-strain curves, the curves' behaviour and the courses fluctuating of each stress-strain curve are pretty similar since the chemical incorporation is the same.

4.3.1.1 Graph Analysis for 0 % Coir Fibre Content

Figure 4.1 shows the axial stress-strain curves of specimens without coir fibre reinforcement on different designated curing periods. Based on the graph, the curve of 56 days curing time has the most prominent peak UCS obtained among all, while the peak UCS gained by the curve of 7 days curing time is the lowest. The peak UCS value arrangement without coir fibre reinforcement of 7 days, 14 days, 21 days, 28 days, and 56 days are 69.66 kPa, 77.33 kPa, 101.30 kPa, 116.49 kPa, and 121.15 kPa, respectively, in ascending order. The gap difference in UCS value between 28 days curing time and 56 days curing time is not that huge. The pozzolanic reaction decreases as curing time goes by, which implies that the strength development nearly complete on the 28^{th} curing day.

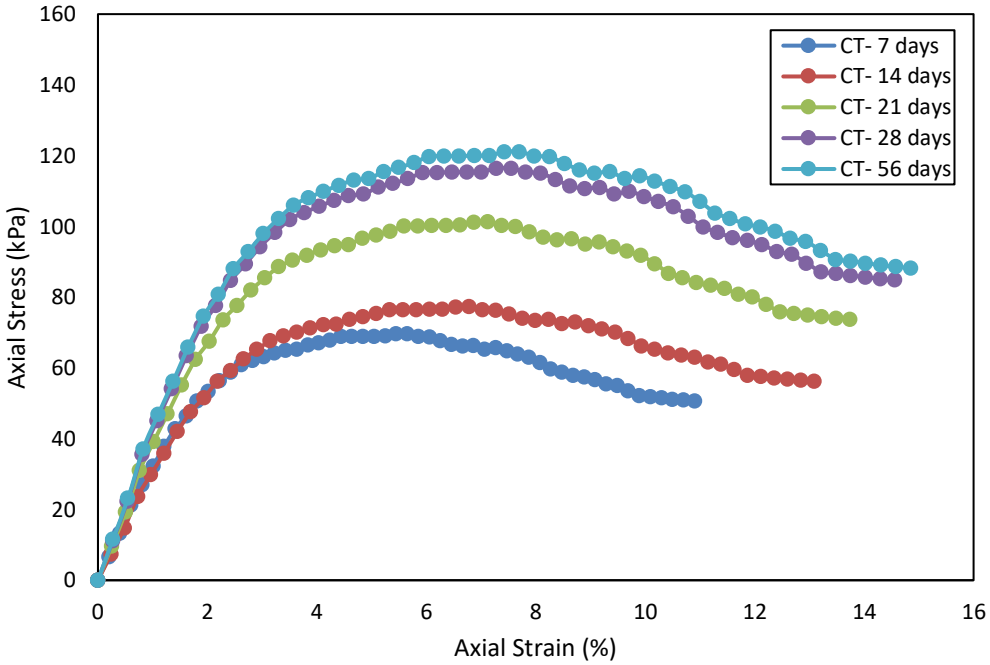

Figure 4.1: Stress-Strain Curve of UCT for 0 % Coir Fibre.

4.3.1.2 Graph Analysis for 0.5 % Coir Fibre Content

Figure 4.2 shows the axial stress-strain curves of specimens with 0.5 % of coir fibre reinforcement on five different designated curing period. Based on the graph, the curve of the 56th curing day has the most significant peak UCS obtained among all, while the curve of the 7th curing days had the lowest peak UCS. The peak UCS value in ascending order arrangement with 0.5 % of coir fibre reinforcement of 7 days, 14 days, 21 days, 28 days, and 56 days are 121.91 kPa, 153.61 kPa, 207.37 kPa, 282.02 kPa, and 287.66 kPa, respectively. The UCS of both the 28th curing day and 56th curing day are near each other, and it further implies that the full potential strength development nearly achieves on the 28th curing day. The pozzolanic reaction decreases as curing time extends.

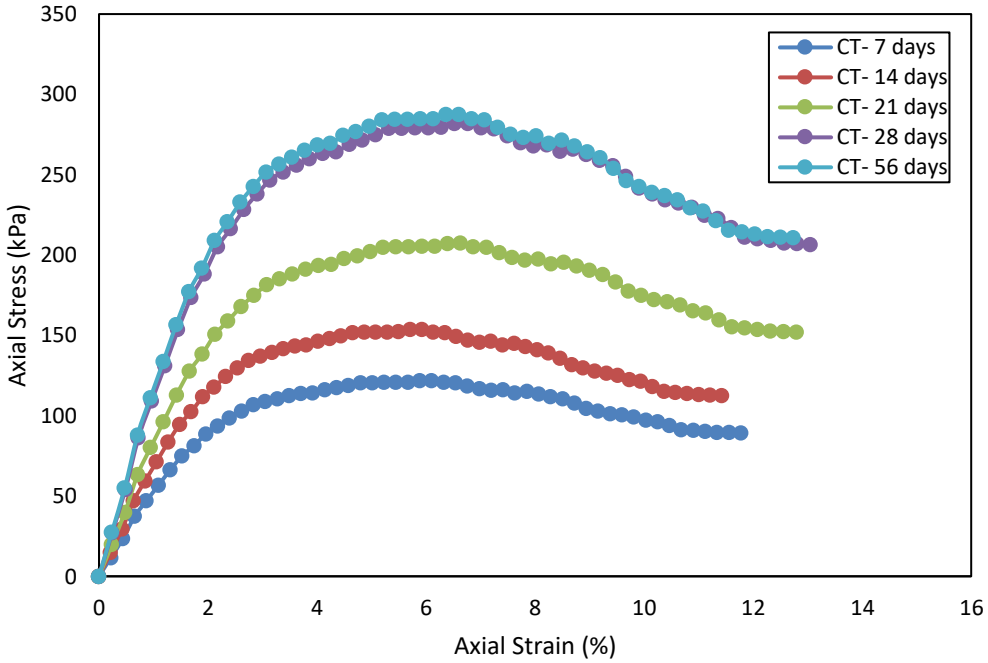

Figure 4.2: Stress-Strain Curve of UCT for 0.5 % Coir Fibre.

4.3.1.3 Graph Analysis for 1.0 % Coir Fibre Content

Figure 4.3 shows the axial stress-strain curves of specimens with 1.0 % of coir fibre reinforcement on five different designated curing period. Based on the graph, the curve of the 56th curing day has the largest peak UCS obtained among all, while the curve of the 7th curing days had the lowest peak UCS. The peak UCS value in ascending order arrangement with 1.0 % of coir fibre reinforcement of 7 days, 14 days, 21 days, 28 days, and 56 days are 230.41 kPa, 324.88 kPa, 396.35 kPa, 495.44 kPa, and 535.07 kPa, respectively. The gap difference in UCS value between the 28th curing day and 56th curing day is not that big. The pozzolanic reaction decreases as curing time extends, which denote that the strength development nearly complete on the 28th curing day.

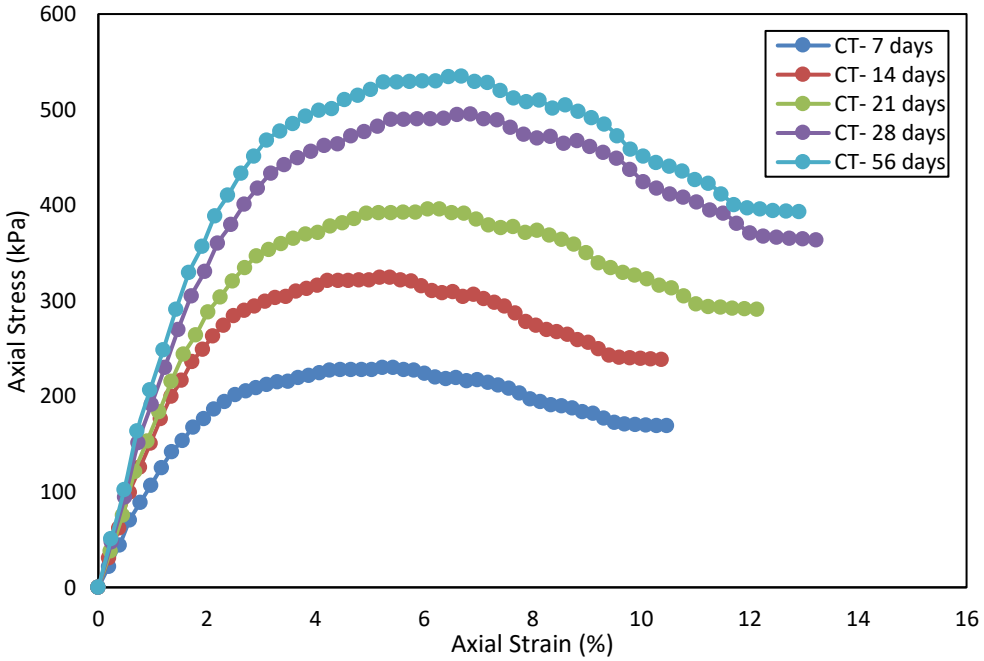

Figure 4.3: Stress-Strain Curve of UCT for 1.0 % Coir Fibre.

4.3.1.4 Graph Analysis for 1.5 % Coir Fibre Content

Figure 4.4 shows the axial stress-strain curves of specimens with 1.5 % of coir fibre reinforcement on five different designated curing period. Based on the graph, the curve of the 56th curing day has the largest peak UCS obtained among all, while the curve of the 7th curing days had the lowest peak UCS. The peak UCS value in ascending order arrangement with 1.0 % of coir fibre reinforcement of 7 days, 14 days, 21 days, 28 days, and 56 days are 165.90 kPa, 195.76 kPa, 309.29 kPa, 411.36 kPa, and 460.72 kPa, respectively. The gap difference in UCS value between the 28th curing day and 56th curing day is comparatively low to others. The pozzolanic reaction decreases as curing time extends, which conveys that the strength development is almost complete on the 28th curing day.

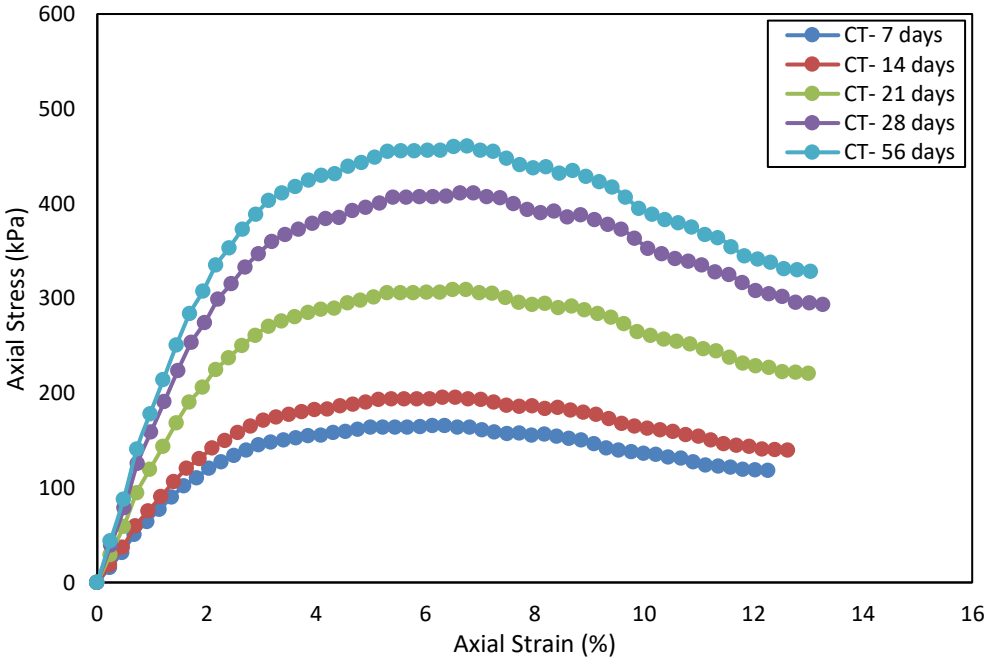

Figure 4.4: Stress-Strain Curve of UCT for 1.5 % Coir Fibre.

4.3.2 Variation of Unconfined Compressive Strength at Different Fibre Content

Figure 4.5 displays the unconfined compressive strength of the treated specimens. As shown in the figure, the UCS of the specimens is influenced by the reinforcing fibre content at different percentages implementation. By looking into the plotting with respective curing time separately, the value of UCS increases as the coir fibre content increases. Each of the separate plotting lines holds a very much alike in graph's behaviour. The UCS values increase gradually until it reaches the peak value and starts to decrease to a particular value. Besides that, when comparing the UCS values of different curing periods at the same reinforcing coir fibre content, it indicates that the values of UCS improve with the extended curing period. Such indication is due to the time-factor control and self-hardening characteristic to the strength development. While the fibre content is at 1 %, five groups of different curing period on 7th, 14th, 21st, 28th, and 56th achieve the peak values of 230.41 kPa, 324.88 kPa, 396.35 kPa, 495.44 kPa, and 535.07 kPa, respectively. The highest peak value of the lime-fly ash-sodium silicate mixes specimen with 1 % of coir fibre reinforcement is 535.07 kPa on the 56th curing day. Also, coir fibre

reinforcement at 1 % serves a higher developing strength than reinforcing fibre content or curing period.

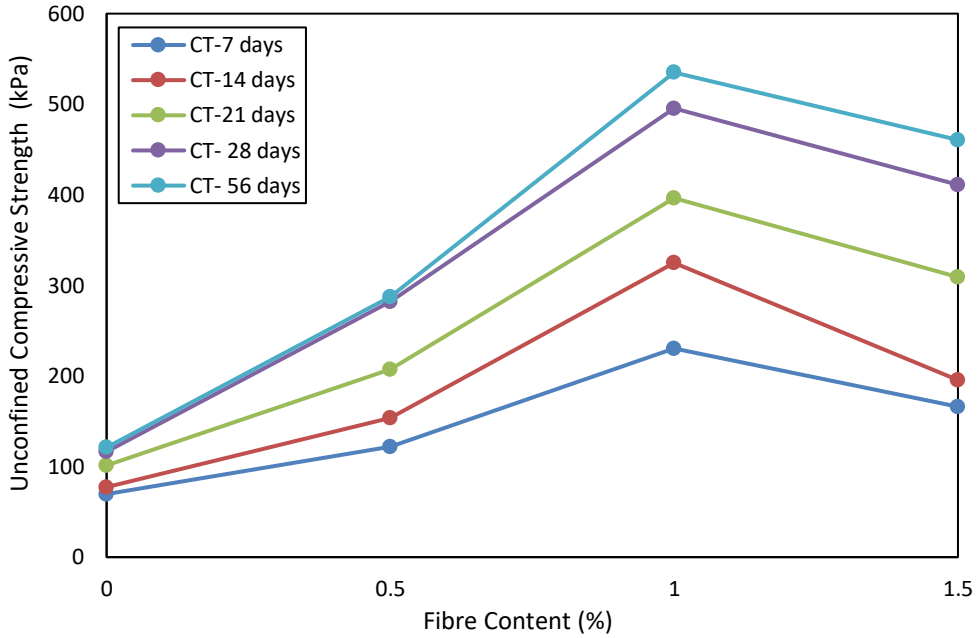

Figure 4.5: Unconfined Compressive Strength (UCS) of Specimens with Different Fibre Content.

4.3.3 Unconfined Compressive Strength Improvement in Percentages

Figure 4.6 exhibits the UCS improvement of specimens in percentages with different fibre content reinforcement. The chemically-treated specimens yet without coir fibre reinforcement are noted as a base reference, and it justifies the zero value for UCS improvement at 0 % of fibre reinforcement as the display in Figure 4.6. The illustration of this column chart provides a good way to present the percentages of UCS improving with different fibre content reinforcement on various designated curing period. As shown in the column chart, the specimens with 1 % reinforcing fibre have greater UCS improved percentages. Other than that, UCS improvement on both the 28th curing day and 56th curing day generally show better strength development. It can be further indicating that the 28th curing day is an optimum curing period since the strength development of the 28th curing day is very much close to the 56th curing day. Furthermore, sand stabilization on the 28th curing day yields a desirable strength developing progress while shortening any time-demanding activities such as

field-stabilizing purposes, experimental aspect, construction site, etc. The UCS of specimens reinforced with fibre content at 1 % for curing period on 7th, 14th, 21st, 28th, and 56th are 230.76 %, 320.12 %, 291.26 %, 325.31 %, and 341.66 %, respectively. As shown in Figure 4.6, the highest value of strength improvement among all other groups is 341.66 % on the 56th curing day while having 1 % of coir fibre reinforcement.

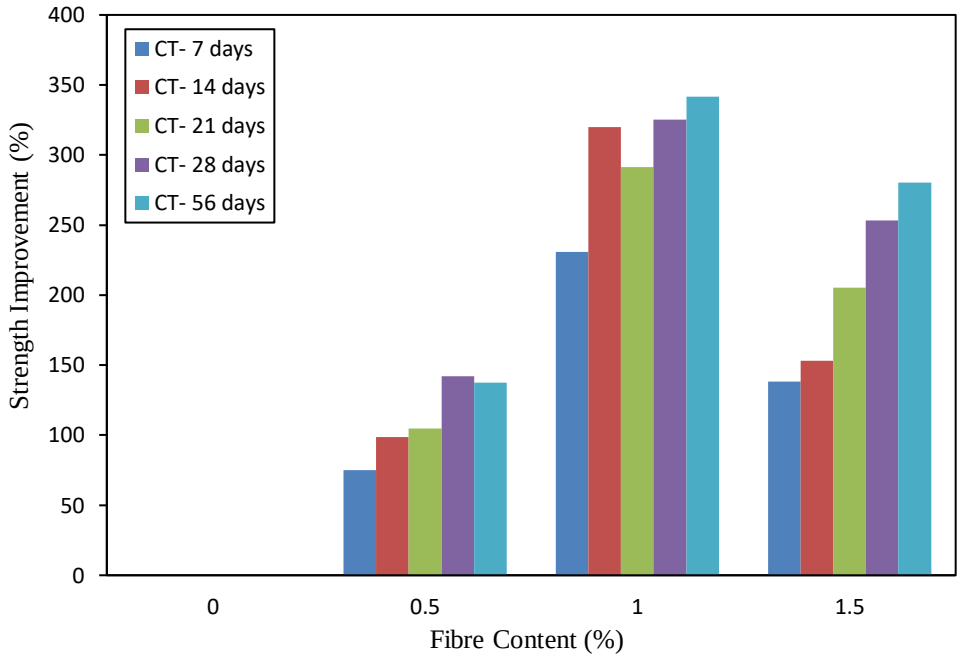

Figure 4.6: Percentages of Unconfined Compressive Strength (UCS) Improving of Specimens.

4.4 Direct Shear Strength

The direct shear test was used to determine the shear strength geotechnical properties of the sand specimens, such as the cohesion and internal friction angle. Table 4.4 shows the results of sand specimens in direct shear test, and the untreated specimen S0 that tagged with 0 kPa and 30.20° of the angle of internal friction has been taken as a base reference. The cohesion of all the chemical treated and coir fibre reinforced specimens was enhanced, especially for those with 1 % coir fibre reinforcement. The cohesion value of specimens reinforced with fibre content 0 %, 0.5 %, 1.0 %, and 1.5 % are 6.25 kPa, 10.73 kPa, 15.77 kPa, and 14.65 kPa, respectively, on the 7th curing day. The specimen S19 with 1 % coir fibre-5 % lime-25 % fly ash-1 % sodium silicate-sand mix has the

highest cohesion value of 96.43 kPa on the 56th curing day. The angle of internal friction of specimens was noticeably influenced, and treated specimens have a higher internal friction angle than the base reference.

Table 4.4: Direct Shear Strength of Sand Specimens.

Specimens	Dry density (g/ cm^3)	Coir fibre (%)	Cohesion (kPa)	Angle of internal friction (°)	Curing period, CT (days)
S0	1.52	0	0	30.20	-
S1	1.52	0	6.25	30.43	7
S2	1.52	0.5	10.73	31.90	
S3	1.52	1.0	15.77	33.48	
S4	1.52	1.5	14.65	28.5	
S5	1.52	0	21.92	30.30	14
S6	1.52	0.5	24.37	33.24	
S7	1.52	1.0	25.38	34.92	
S8	1.52	1.5	18.38	31.88	
S9	1.52	0	30.52	33.24	21
S10	1.52	0.5	34.78	33.74	
S11	1.52	1.0	38.58	36.65	
S12	1.52	1.5	36.76	31.93	
S13	1.52	0	48.32	34.04	28
S14	1.52	0.5	59.26	35.52	
S15	1.52	1.0	69.11	37.15	
S16	1.52	1.5	52.34	32.63	
S17	1.52	0	84.23	36.14	56
S18	1.52	0.5	90.38	36.89	
S19	1.52	1.0	96.43	42.00	
S20	1.52	1.5	73.02	36.65	

4.4.1 Cohesion of Sand Specimens

Figure 4.7 depicts the alterations of cohesion with different fibre content expressed as percentages by the weight of sand specimen regarding curing period. The cohesion of the specimen enhances as the fibre content increases to a particular value; also, it shows a shear strength reduction in cohesion when there is a further addition of fibre content that exceeds 1 %. With the same chemical mixture, the specimens with 1 % fibre content reinforcement comparatively built a much higher cohesion value overall. Moreover, it can be observed that there was a significant cohesion values improvement by comparing the specimens with varied curing period at 0 % fibre content. At 0 % fibre content, it can be said that specimen S1, S5, S9, S13, and S17 had a positive strength development which further indicates that lime-fly ash-sodium silicate mixes without fibre content inclusion yield a cohesion increment, and it has been contributed by curing time as a factor. While the fibre content is 1 %, the specimens' peak cohesion with the curing period of 7 days, 14 days, 21 days, 28 days, and 56 days were 15.77 kPa, 25.38 kPa, 38.58 kPa, 69.11 kPa, and 96.43 kPa, respectively. The graph behaviour shows most likely the same for the cohesion value in each designated curing time. The specimen reinforced with 1 % fibre content had reached the highest cohesion value of 96.43 kPa on the 56th curing days.

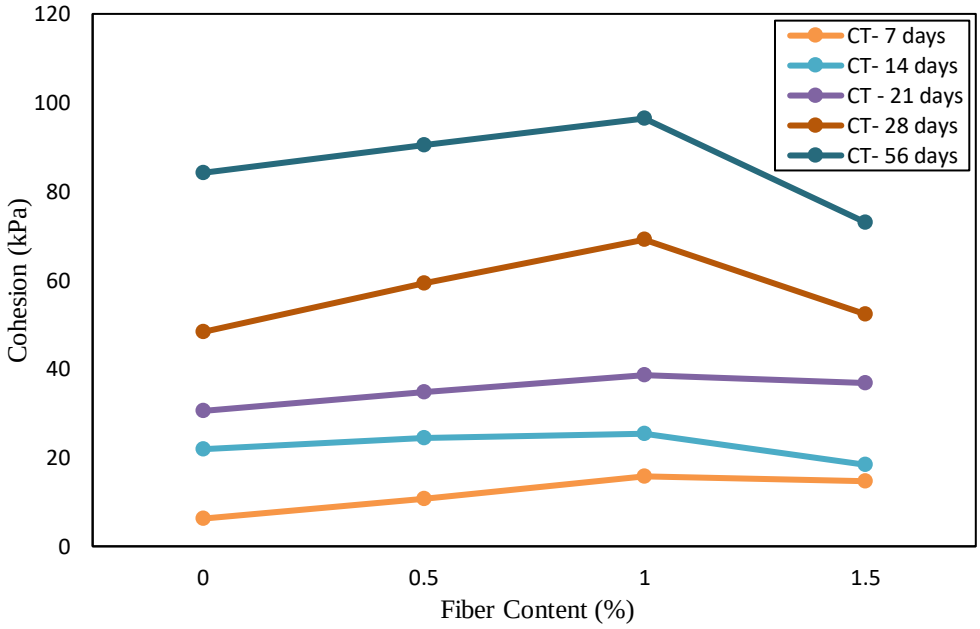

Figure 4.7: Graph of Cohesion of Sand Specimens with Different Fibre Content.

4.4.2 Angle of Internal Friction of Sand Specimens

Figure 4.8 represents the variations for specimens' angle of internal friction reinforced with different fibre content while considering the curing period. Based on the graph observation, it is sighted that the angle of internal friction was disturbed by the percentage of fibre content added into the specimens and the extension of the curing time. The base reference of specimen S0 has a 30.20° angle of internal friction, as stated in Table 4.4. The angle of internal friction for each specimen increases as the fibre content increases. The graph also indicates that the angle of internal friction had declined when specimens were reinforcing beyond 1.0 % fibre content. At 1 % fibre content reinforcement, specimen S3, S7, S11, S15, and S19 reached their respective peak angle of internal friction, although the curing period was different.

Besides, comparing the specimens with the angle of internal friction at 0 % fibre content determines that lime-fly ash-sodium silicate mixes aid the frictional angle formation for soil failure encounter to shearing stress. The curing time also supported the shear strength development and was raising the angle of internal friction. While the fibre content is 1 %, the best angle of internal friction of the specimens with the curing period of 7 days, 14 days, 21 days, 28 days, and 56 days were 33.48°, 34.92°, 36.65°, 37.15°, and 42.00°, respectively. The graph shows a similar trending of inclination for each curing time, ranging from 0 to 1 % fibre content and declination afterwards of fibre content addition. The specimen reinforcing with 1 % fibre content had reached the highest value of 42.00° angle of internal friction on the 56^{th} curing day. The presence of a suitable percentage of fibre content can advance the soil's cohesion and angle of internal friction.

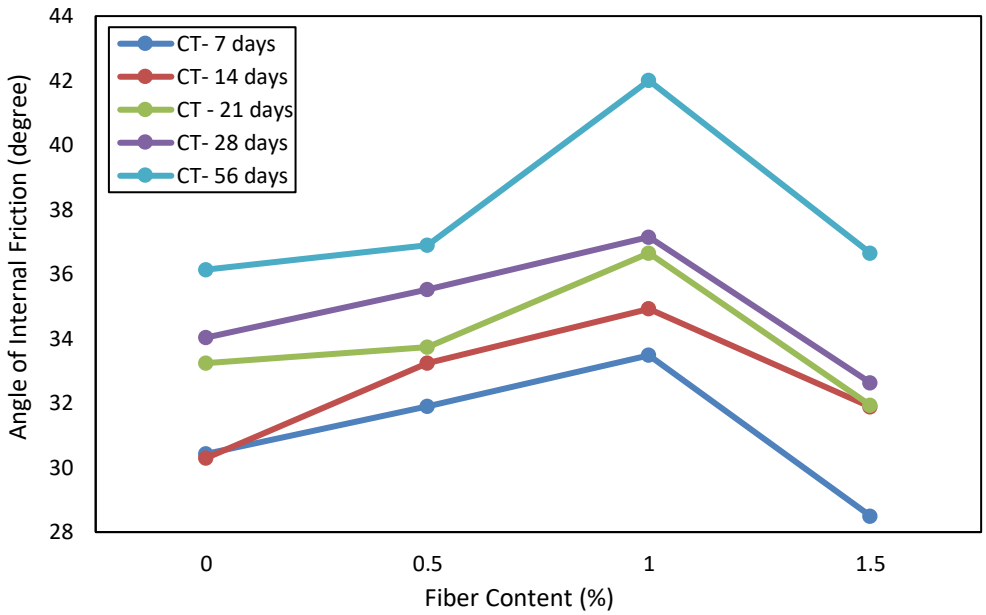

Figure 4.8: Angle of Internal Friction of Sand Specimens with Different Fibre Content.

4.5 Effect of Lime-Fly Ash-Sodium Silicate Mix along with Curing Period

The lime-fly ash's involvement binds the sand grains, forming a matrix among the sand particles and filling up the voids, subsequent into bigger particles and better strength properties. Such strength development is the outcome of the cementitious reaction, pozzolanic reaction, and the placement of self-hardening characteristic during the curing period. The enhancement of the specimen's mechanical properties is owing to the chemical reaction and fibre mechanism endured over the curing period (Simatupang, et al., 2020; Krithiga, et al., 2016; Jawad, et al., 2014). Moreover, as referring to the stress-strain curves under sub-subsection 4.3.1, there is an alleviation of stress after the curve reaching the peak value where failure starts; such happening indicates the brittle behaviour of the bonding contributed by fly ash content within the specimen. The silica and alumina reaction from fly ash with the dissolved lime forms the calcium aluminate hydrate (C-A-H) and calcium silicate hydrate (C-S-H). C-S-H gel is a cohesive-frictional substance with strength asymmetry in compression and tension, and normal-stress dependence with maximal shear strength (Simatupang, et al., 2020).

When it comes to the stress-strain relationship, the shear strength of the fly-ash-stabilized sands follows the same pattern as the compressive strength in terms of improvement rate. During the curing process, the formed bond undergoes self-hardening, resulting in a much stronger specimen. Also, the shear strength of the specimen with the treat of lime-fly ash is greater than that of the untreated specimen, as shown in Table 4.4, since a more prominent grain holds a higher angle of internal friction. Furthermore, a stronger specimen has a direct effect on cohesion improvement. As shown in Figure 4.8, the shear strength of stabilized sands will drop near to or even lower than the residual shear strength if it is sheared further and exceeds the strength limit. Such a drawback is mainly due to the deteriorating and weakening of the bond formation (Simatupang, et al., 2020).

Based on Figure 4.6, by comparing the intensity of each column of strength improvement at the same reinforcing fibre content, it can describe the curing period's impact on the strength development of the stabilized specimens at different curing stages. As seen in the figure, the longer the curing period will result in a much more significant UCS improvement of the specimen. Other than that, under the concerns about the progression of curing time on Figure 4.7 and Figure 4.8, both figures present a significant improvement in shear strength parameters of both cohesive strength and angle of internal friction. The cohesion increases around six times the value from the curing period of 7 days to 56 days. The main factor is the self-hardening of the mixture between lime-fly ash and sand particles, whereas the origination of cementitious compounds (C-S-H and C-A-H) formation due to the pozzolanic reaction (Simatupang, et al., 2020).

In soil stabilization, soil particles often rotate in the fibre-soil interface, leading to specific weak bonding between the soil hardening formation and the inability to raise the full potential of strength development. Such rotation appears within the fibre-soil interface, and yet the implementation of sodium silicate stabilization in this study imposed a bonding force between the soil particles to limit such rotation. Also, the benefits of using sodium silicate are soil-rotating limitation, better bond formation, strength enhancement, and short aid in the rate of curing progress (Shukla, 2017).

4.6 Fibre Reinforcement Mechanism

The process of strength mobilization in fibre reinforced soils is attributable to the fibres' tensile resistance, supported by the tight bonding between fibres and soil. The loose structure of unreinforced specimen S0 is due to the 0 kPa cohesion value between the sand particles. The experimental results for specimen S1, S5, S9, S13, and S17 shown in Table 4.4 are labelled comparatively with low cohesion and inferior angle of internal friction by reviewing the graph tendency in Figure 4.7 and Figure 4.8. When diving into the structure's inner sight, the fibre reinforcement system primarily consists of the coir fibre and sand particles constraining with each other to create interface force. This interface force's primary cause gives rise to the extrusion pressure appear through cohesion and frictional angle (Liu, et al., 2018).

In the aspect of UCS behaviour, as shown in Figure 4.5, the strength development of specimens was owing to the enrollment of tensile resistance by fibres associated with high interfacial force at the fibre-matrix interface, which it is deriving from physicochemical and mineralogical modification in the course of pozzolanic reactions within the treated specimens. It is reasonable to assume that fibre adhesion to soil increased during the curing period. In the direct shear test, the fibre reinforced sand easily forms a three-dimensional fibre-sand net under confining stress. When fibre content is limited inside the specimen, ample spacing between the fibres plus the less physical interaction of fibre and sand makes it much more difficult to shape an efficient net between fibre and sand (Liu, et al., 2017). Thus, less attachment and poor arrangement of the fibre content offer a little support in strength development yet not with a practical approach.

On the other hand, as the fibre content increases steadily, the fibres have more sharing and interacting surface area to allow neighbouring fibres to quickly converge, forming an efficient fibre-sand net that improves cohesion and angle of internal friction. In such an event, the friction between fibre and sand particles increases as the interface between fibre and sand particles expands. Furthermore, as local cracks occur in soil, fibres around the cracks absorb the soil's tensile stress by fibre-soil friction, thereby avoiding further crack growth and improving the soil's resistance to the force applied as the UCS of soil (Liu, et al., 2017).

However, more fibre filaments will be collecting in clusters within the sand sample if the fibre content is getting much higher than exceeds the optimum ratio, resulting in a non-uniform distribution of fibres and imperfect contact of fibre and sand particles. In addition, uneven fibre distribution and poor orientation minimize the macro interactions between fibres and soil, lowering the fibres' tensile strength mobilization potential. It is possible to form a vulnerable region of strain that weakens the strength enhancement progress due to excessive fibre content (Liu, et al., 2017). As a result, specimens experienced an inevitable reduction in the efficiency of improving compressive strength and shear strength parameters. Based on Figure 4.5, Figure 4.7 and Figure 4.8, all the values of UCS, cohesion and angle of internal friction of treated specimens improve concurrently with the increment of fibre content but decrease when the fibre content was approaching 1.5 %. In such a case, 1 % of fibre content involvement may presume as an optimum ratio for this testing aspect.

It can be concluded that the different content of coir fibre reinforcement and duration of the curing period will affect the rate of strength improvement and strength development progress. The strong formation of framework structure is much more complete with the increase of fibre content. Nonetheless, an excessive fibre content reinforcement will doubtlessly pose in clusters after the complete formation of framework structure and lead to an occurrence that pozzolanic gel is tough to enwrap the surface area of the fibre content entirely to form a whole stable structure. As a result, the UCS increases as the fibre content increases. Meanwhile, after the fibre content is more than 1.0 %, the UCS decreases as the fibre content increases. The cohesion and angle of internal friction increase as the fibre content increases; after the reinforcing fibre content exceeds 1 %, the cohesion and angle of internal friction decreases as the fibre content increases. The strength development is much more significant with a more extended curing period. Thus, the UCS, cohesion, and angle of internal friction increase with the increase of fibre content and the curing period for the specimens.

4.7 Summary

The result analysis and discussion based on the experimental study have been accomplished throughout this chapter. This chapter has been discussing the outcome of geotechnical properties of the non-stabilized and stabilized sand specimens with the combination mix of reinforcing coir fibre-lime-fly ash-sodium silicate-sand. In this study, the specimen's combination is a fixed proportion of 5 % of lime, 25 % of Class C fly ash, 1 % of sodium silicate while having the different incorporating measure of coir fibre content with 0 %, 0.5 %, 1.0 %, and 1.5 %. The designated curing period of 7 days, 14 days, 21 days, 28 days, and 56 days has been performed to determine the specimens' strength development. The strength improvement percentage rate of the 1 % reinforcing fibre content is ranged from 230.76 % to 341.66 % for the unconfined compression test. The unconfined compressive strength value of the 1 % reinforcing fibre content is ranged from 230.41 kPa to 535.07 kPa. The highest result obtained is 535.07 kPa of UCS with a 341.66 % improving rate on the 56^{th} curing day. For the direct shear strength, the highest shear strength parameters of cohesion and angle of internal friction achieved are 96.43 kPa and 42.00°, respectively, with the 56 days of curing period. Based on both laboratory tests, 1 % of coir fibre reinforcement on the stabilized sand specimens yields effective and significant strength enhancement on the 56^{th} curing day. However, the curing period of 28 days is a considerable curing duration since the geotechnical properties of the 28^{th} curing period yield a desirable outcome yet with a shorter time frame. Moreover, the specimen's fibre reinforcement mechanism has been explained thoroughly, and the 1 % reinforcing fibre provides an excellent fibre-soil interface and stable structure.

CHAPTER 5

CONCLUSION AND RECOMMENDATION

5.1 Conclusion

Unconfined compression test and direct shear test on the stabilized sand specimens with different coir fibre content and curing period were conducted to examine the unconfined compressive strength and shear strength parameter. The test outcomes, as well as the reinforcement mechanism, were examined. The key findings can be outlined as follows based on the outcomes of the experiments:

1. The reinforced coir fibre-lime-fly ash-sodium silicate-sand mixing combination content will significantly increase the unconfined compressive strength (UCS) of the sand sample. The UCS of the stabilized sand specimen increases as the coir fibre content increases but shows downward behaviour when the coir fibre further increases beyond 1 % of fibre reinforcement. The time factor of curing duration will potentially increase the UCS under the same fibre content proportion. The specimen reinforced with 1 % of coir fibre content has obtained a most outstanding UCS value of 535.07 kPa. The highest UCS improvement percentage is 341.66 %. The curing period of 56 days yields the best strength development.
2. The fibre reinforced combination increases the shear strength parameters of both cohesive strength and angle of internal friction; the cohesive strength and the angle of internal friction of the specimen increase as the coir fibre content increases. The declination manner occurs on both shear strength parameters when there is an excessive reinforcing fibre amount. The highest achieved value for cohesive strength and angle of internal friction of the specimen is 96.43 kPa and 42.00°, respectively, while having coir fibre reinforcement of 1 % proportion. All stabilized specimens have better shear strength parameters than the unstabilized specimens.

3. In terms of the mechanism of reinforced coir fibre-lime-fly ash-sodium silicate-sand mixture, the coir fibre serves as the matrix and is scattered across the sand particles, while pozzolanic gel fills up the voids and binds up the sand particles and fibre-sand interface. The pozzolanic gel enwraps the sand particles and coir fibre, allowing them to form tightly together as an intact structure to enhance the geotechnical properties. The project findings can be used as a guide for practical engineering such as the foundation, embankment, landfill reinforcement, etc.

5.2 Recommendations

The study of the reinforced coir fibre-lime-fly ash-sodium silicate-sand mixture with varying fibre content proportion is still limited in this field. Therefore, recommendations and suggestions ought to be taken into consideration to improve the specifications of the further studies:

1. A higher water-to-sand weight ratio is recommended with a smaller interval to determine the optimum moisture content for a reinforced coir fibre-lime-fly ash-sodium silicate-sand mixture during the mixing procedure.
2. Attempt different laboratory tests such as the triaxial test and California Bearing Ratio (CBR) test. Such an attempt might investigate the geotechnical properties and characteristics of reinforced coir fibre-lime-fly ash-sodium silicate-sand mixture in a much comprehensive manner.
3. Scanning Electron Microscopy (SEM) test is recommended to scan the specimen with an electron beam to capture a magnified high-resolution image for analysis. The SEM analysis can be helpful in microstudy and evaluation for surface fractures and flaws, etc.

REFERENCES

Ahmed, L.A.J. and Radhia, M., 2019. Sandy Soil Stabilization with Polymer.

Al-Swaidani, A., Hammoud, I. and Meziab, A., 2016. Effect of adding natural pozzolana on geotechnical properties of lime-stabilized clayey soil. *Journal of Rock Mechanics and Geotechnical Engineering*, *8*(5), pp.714-725.

Bahar, R., Benazzoug, M. and Kenai, S., 2004. Performance of compacted cement-stabilized soil. *Cement and concrete composites*, *26*(7), pp.811-820.

Baldovino, J.D.J.A., dos Santos Izzo, R.L., Moreira, E.B. and Rose, J.L., 2019. Optimizing the evolution of strength for lime-stabilized rammed soil. *Journal of rock mechanics and geotechnical engineering*, *11*(4), pp.882-891.

Bareither, C.A., Benson, C.H. and Edil, T.B., 2008. Comparison of shear strength of sand backfills measured in small-scale and large-scale direct shear tests. *Canadian Geotechnical Journal*, *45*(9), pp.1224-1236.

Buhler, R.L. and Cerato, A.B., 2007. Stabilization of Oklahoma expansive soils using lime and class C fly ash. In *Problematic soils and rocks and in situ characterization* (pp. 1-10).

Cheng, Y., Wang, S., Li, J., Huang, X., Li, C. and Wu, J., 2018. Engineering and mineralogical properties of stabilized expansive soil compositing lime and natural pozzolans. *Construction and Building Materials*, *187*, pp.1031-1038.

Craig, R.F., 2004. *Craig's soil mechanics*. CRC press.

Eisazadeh, A., 2010. *Physicochemical behaviour of lime and phosphoric acid stabilized clayey soils* (Doctoral dissertation, Universiti Teknologi Malaysia).

Garber, N.J. and Hoel, L.A., 2009. Traffic and highway engineering.: Cengage Learning.

Hafez, M.A., Sidek, N. and Noor, M.M., 2008. Effect of pozzolanic process on the strength of stabilized lime clay. *Electron. J. Geotech. Eng.*, *13*, pp.1-19.

Haghi, A.K., Arabani, M. and Veis Karami, M., 2006. Applications of expanded polystyrene (EPS) beads and polyamide 66 in civil engineering, Part Two: Stabilization of clayey sand by lime/polyamide-66. *Composite Interfaces*, *13*(4-6), pp.451-459.

Harichane, K., Ghrici, M. and Kenai, S., 2011. Effect of curing time on shear strength of cohesive soils stabilized with combination of lime and natural pozzolana.

Holt, C., 2010. Chemical Stabilization of Inherently Weak Subgrade Soils for Road Construction–Applicability in Canada. In *Annual Conference of the Transportation Association of Canada Halifax, Nova Scotia*.

Huat, B.B., Maail, S. and Mohamed, T.A., 2005. Effect of chemical admixtures on the engineering properties of tropical peat soils. *American journal of applied sciences*, *2*(7), pp.1113-1120.

Jamsawang, P., Suansomjeen, T., Sukontasukkul, P., Jongpradist, P. and Bergado, D.T., 2018. Comparative flexural performance of compacted cement-fiber-sand. *Geotextiles and Geomembranes*, *46*(4), pp.414-425.

Jawad, I.T., Taha, M.R., Majeed, Z.H. and Khan, T.A., 2014. Soil stabilization using lime: Advantages, disadvantages and proposing a potential alternative. *Research Journal of Applied Sciences, Engineering and Technology*, *8*(4), pp.510-520.

Joe, M.A. and Rajesh, A.M., 2015. Soil stabilization using industrial waste and lime. *International Journal of Scientific Research Engineering & Technology (IJSRET)*, *4*(7)

Kaniraj, S.R. and Havanagi, V.G., 2001. Behavior of cement-stabilized fiber-reinforced fly ash-soil mixtures. *Journal of geotechnical and geoenvironmental engineering*, *127*(7), pp.574-584.

Kazemian, S., Prasad, A., Huat, B.B., Ghiasi, V. and Ghareh, S., 2012. Effects of cement–sodium silicate system grout on tropical organic soils. *Arabian Journal for Science and Engineering*, *37*(8), pp.2137-2148.

Krithiga, N., Pujitha, D., Palayam, T. and Revathy Sri Muthukumaran, A., 2016. Soil stabilization using lime and fly ash, vol. 08.

Liu, J., Chen, Z., Song, Z., Bai, Y., Qian, W., Wei, J. and Kanungo, D.P., 2018. Tensile behavior of polyurethane organic polymer and polypropylene fiber-reinforced sand. *Polymers*, *10*(5), p.499.

Liu, J., Feng, Q., Wang, Y., Bai, Y., Wei, J. and Song, Z., 2017. The effect of polymer-fiber stabilization on the unconfined compressive strength and shear strength of sand. *Advances in materials science and Engineering*, *2017*.

Ma, Q.Y., Cao, Z.M. and Yuan, P., 2018. Experimental research on microstructure and physical-mechanical properties of expansive soil stabilized with fly ash, sand, and basalt fiber. *Advances in Materials Science and Engineering*, *2018*.

Obuzor, G.N., Kinuthia, J.M. and Robinson, R.B., 2012. Soil stabilization with lime-activated-GGBS—A mitigation to flooding effects on road structural layers/embankments constructed on floodplains. *Engineering Geology*, *151*, pp.112-119.

Olinic, T. and Olinic, E., 2016. The effect of quicklime stabilization on soil properties. *Agriculture and agricultural science procedia*, *10*, pp.444-451.

Rafizul, I.M., Assaduzzaman, M. and Alamgir, M., 2012. The effect of chemical admixtures on the geotechnical parameters of organic soil: a new statistical model. *Journal of Applied sciences and engineering research*, *1*(4), pp.623-634.

Ravindran, G., Isaac, I.A., Olaniyi, D.A., Saravana, K., Murugasamu, M., Sivaraj, G. and Ayyasamy, M., 2019. Banana Fibre-Reinforcement of a Soil Stabilized with Sodium Silicate.

Sadek, S., Najjar, S. and Abboud, A., 2013, September. Compressive strength of fiber-reinforced lightly-cement stabilized sand. In *Proceedings of the 18th International Conference on Soil Mechanics and Geotechnical Engineering, Paris*.

Shukla, S.K., 2017. *Fundamentals of fibre-reinforced soil engineering*. Singapore: Springer Singapore.

Simatupang, M., Mangalla, L.K., Edwin, R.S., Putra, A.A., Azikin, M.T., Aswad, N.H. and Mustika, W., 2020. The mechanical properties of fly-ash-stabilized sands. *Geosciences*, *10*(4), p.132.

Subramani, T. and Udayakumar, D., 2016. Experimental study on stabilization of clay soil using coir fibre. *International Journal of Application or Innovation in Engineering Management Decision*, *5*, pp.192-204.

Tang, C.S., Wang, D.Y., Cui, Y.J., Shi, B. and Li, J., 2016. Tensile strength of fiber-reinforced soil. *Journal of Materials in Civil Engineering*, *28*(7), p.04016031.

Thyagaraj, T., Rao, S.M., Sai Suresh, P. and Salini, U., 2012. Laboratory studies on stabilization of an expansive soil by lime precipitation technique. *Journal of Materials in Civil Engineering*, *24*(8), pp.1067-1075.

Tingle, J.S., Newman, J.K., Larson, S.L., Weiss, C.A. and Rushing, J.F., 2007. Stabilization mechanisms of non-traditional additives. *Transportation research record*, *1989*(1), pp.59-67.

Vizcarra, G.O.C., Casagrande, M.D.T. and da Motta, L.M.G., 2014. Applicability of municipal solid waste incineration ash on base layers of pavements. *Journal of materials in civil engineering*, *26*(6), p.06014005.

Ye, B., Z. R. Cheng, C. Liu, Y. D. Zhang, and P. Lu. "Liquefaction resistance of sand reinforced with randomly distributed polypropylene fibres." *Geosynthetics International* 24, no. 6 (2017): 625-636.

Yixian, W., Panpan, G., Shengbiao, S., Haiping, Y. and Binxiang, Y., 2016. Study on strength influence mechanism of fiber-reinforced expansive soil using jute. *Geotechnical and Geological Engineering*, *34*(4), pp.1079-1088.

Zumrawi, M.M. and Babikir, A.A.A.A., 2017. Laboratory study of steel slag used for stabilizing expansive soil. *University Of Khartoum Engineering Journal*, *6*(2).